

Dynamic crystallization in a quantum Ising chain

K. L. Zhang and Z. Song*
School of Physics, Nankai University, Tianjin 300071, China

The topological degeneracy of ground states in transverse field Ising chain cannot be removed by local perturbation and allows it to be a promising candidate for topological computation. We study the dynamic processes of crystallization and dissolution for the gapped ground states in an Ising chain. For this purpose, the real-space renormalization method is employed to build effective Hamiltonian that captures the low-energy physics of a given system. We show that the ground and first-excited eigenstates of an $(N + 1)$ -site chain can be generated from that of the N -site one by adding a spin adiabatically and vice versa. Numerical simulation shows that the robust quasi-degenerate ground states of finite-size chain can be prepared with high fidelity from a set of non-interacting spins by a quasi-adiabatic process. As an application, we propose a scheme for entanglement transfer between a pair of spins and two separable Ising chains as macroscopic topological qubits.

I. INTRODUCTION

The transverse field Ising model is a paradigm in both traditional second-order quantum phase transition (QPT) based on spontaneous symmetry breaking [1] and topological QPT, which is immune to local perturbation [2, 3]. One of the remarkable features of the one-dimensional Ising chain is that its topological degenerate ground states are protected from higher energy excitations by the energy gap, and are characterized by the existence of Majorana edge states, which are robust to perturbations [4]. In the past few decades, the numerical calculations [5–10] and experimental investigation [11–13] in quasi-one-dimensional complex compounds triggered the study of macroscopic quantum phenomena in quantum spin systems [14, 15]. It has been reported that an interacting Ising spin chain can be simulated by using a Mott insulator spinless bosons in a tilted optical lattice [16]. And it is similar to the ground states of spin-1 antiferromagnetic Heisenberg chain, which possesses a topological phase of matter known as the Haldane phase [17–19]. A promising application of such quantum spin systems is physical implementation of quantum information processing devices based on solid state system [20–24]. Thanks to the intrinsic stability of the topological feature, a system with topological phase can be a promising platform for quantum computation and information processing [25–27]. It motivates us to develop an alternative candidate for macroscopic qubit based on the Ising chain in the topological phase, due to the fact that its degenerate ground states are robust against the disordered perturbation.

In this work, we explore a way to prepare the ground state and first-excited state of an Ising chain on demand by dynamic process of crystallization, generating robust macroscopic quantum states against disordered perturbation. Based on an analytic perturbation analysis, we employ a real-space renormalization method to build ef-

fective Hamiltonian that capture the low-energy physics of a given system. Within the topologically nontrivial region, the effective Hamiltonian for an $(N + 1)$ -site chain is obtained from ground and first-excited states of an N -site chain. It is a modified two-spin Ising model, which is exactly solvable and allows one to design an adiabatic passage for crystallization or dissolution. We show that the ground and first-excited states of an $(N + 1)$ -site chain can be generated from that of the N -site one by adding a spin adiabatically and vice versa. Starting from $N = 1$, as a seed crystal, numerical simulation is performed for quasi-adiabatic process, confirming our prediction. As an application in quantum information processing, we demonstrate the scheme of entanglement transfer between a pair of qubits and two Ising chains, as macroscopic objects.

This paper is organized as follows. In Sec. II, we present the model and its symmetries. In Sec. III, an effective Hamiltonian that capture the low-energy physics is obtained based on a real-space renormalization method. In Sec. IV, we propose an adiabatic passage for crystallization, which generates the ground and first-excited states of finite-size chain from simple spin configurations. It allows the scheme of entanglement transfer from two qubits to two Ising chains, creating a macroscopic entangled state. In Sec. V, we investigate the robustness of the ground states in the presence of quenched disordered perturbation. We also propose an adiabatic passage for entanglement distillation from an obtained macroscopic entangled state. Section VI summarizes the results and explores its implications.

II. MODEL AND SYMMETRIES

We consider the Hamiltonian of a transverse field Ising model

$$H = \sum_{j=1}^{N-1} J_j \sigma_j^x \sigma_{j+1}^x + \sum_{j=1}^N g_j \sigma_j^z, \quad (1)$$

* songtc@nankai.edu.cn

on a chain with open boundary condition, where σ_j^α ($\alpha = x, y, z$) are the Pauli operators on site j and parameters J_j and g_j are position and time dependent, without losing the generality. The second term and quantity $\sigma^z = \sum_{j=1}^N \sigma_j^z$ have common eigenstates, and the first term breaks the conservation of this quantity. However, the parity of the eigenvalue of σ^z is conservative, i.e., we always have

$$[p, H] = 0, \quad (2)$$

where the parity operator

$$p = \prod_{j=1}^N (-\sigma_j^z). \quad (3)$$

We start with the simple case with uniform parameters, $J_j = J$ and $g_j = g$, to analyze the property of the ground state. For finite N , the parity of ground state with non-zero g can be determined by the ground state in $g = \pm\infty$ limit. It is due to the fact of non-degeneracy of the ground state for finite N and nonzero g . Actually, it has been shown that the spectrum of H can be constructed based on the positive levels of the corresponding Su-Schrieffer-Heeger (SSH) chain [4]. The non-zero energy levels of an SSH chain results in the fact that the ground state energy is non-degeneracy except at $g = 0$ (or infinite N with $|g/J| < 1$). Here we give the conclusions of the parity of ground state: (i) for even N , we have $p = 1$ for the ground state with any $g \neq 0$, while (ii) for odd N , we have $p = \text{sgn}(g)$.

For a finite N system with periodic boundary condition, the exact solution can be obtained and the ground state obeys the same rule. It is the common sense that the property of the model is not sensitive to the boundary condition in thermodynamic limit. Nevertheless, here we would like to emphasize that the Hamiltonian with $|g/J| < 1$ and infinite N possesses an exclusive symmetry. It can be check that there exist a nonlocal spin operator (see Appendix)

$$D_N = \frac{1}{2} \sqrt{1 - \left(\frac{g}{J}\right)^2} \sum_{j=1}^N \prod_{l < j} (-\sigma_l^z) \times \left[\left(-\frac{g}{J}\right)^{j-1} \sigma_j^x - i \left(-\frac{g}{J}\right)^{N-j} \sigma_j^y \right], \quad (4)$$

satisfying the commutation relations

$$[D_N, H] = [D_N^\dagger, H] = 0, \quad (5)$$

$$\{D_N, D_N^\dagger\} = 1, (D_N)^2 = (D_N^\dagger)^2 = 0, \quad (6)$$

We would like to point out that the commutation relation in Eq. (5) can be regarded as a symmetry of the system. Importantly, such a symmetry is conditional, requiring $|g/J| < 1$, large N limit and open boundary. The first two conditions accords with the symmetry breaking mechanism for QPT [1].

Furthermore, the commutation relation in Eq. (5) guarantee the existence of degeneracy of the eigenstates. There might be a set of degenerate eigen states $\{|\psi_n^+\rangle, |\psi_n^-\rangle\}$ of H with eigen energy E_n , in two invariant subspaces, i.e.,

$$H |\psi_n^\pm\rangle = E_n |\psi_n^\pm\rangle \quad (7)$$

and

$$p |\psi_n^\pm\rangle = \pm |\psi_n^\pm\rangle. \quad (8)$$

Importantly, we have the relations

$$D_N |\psi_n^+\rangle = |\psi_n^-\rangle, D_N^\dagger |\psi_n^-\rangle = |\psi_n^+\rangle, \\ D_N^\dagger |\psi_n^+\rangle = D_N |\psi_n^-\rangle = 0. \quad (9)$$

Especially, applying the operator D_N (D_N^\dagger) on the lowest energy eigenstates $|\psi_g^+\rangle$ and $|\psi_g^-\rangle$ of H in two invariant subspace, we have

$$D_N |\psi_g^+\rangle = |\psi_g^-\rangle, D_N^\dagger |\psi_g^-\rangle = |\psi_g^+\rangle, \\ D_N^\dagger |\psi_g^+\rangle = D_N |\psi_g^-\rangle = 0, \quad (10)$$

and then $|\psi_g^+\rangle$ and $|\psi_g^-\rangle$ are degenerate ground states. In the rest of this paper, we denote eigenstates $|\psi_g^+\rangle$ and $|\psi_g^-\rangle$ by $|\psi_g^N\rangle$ and $|\psi_e^N\rangle$, representing the ground and first-excited states, respectively.

Such a symmetry is also responsible for the topological degeneracy. In fact, there also exists an operator D_N for the Hamiltonian in the presence of slight disordered deviations on the uniform $J_j = J$ and $g_j = g$, since the edge mode of SSH chain is robust against disordered perturbation (see Appendix). Thus the degeneracy of ground sates cannot be lifted by local perturbation. It is desirable to employ such two states as two orthonormal basis states of a topological qubit. To this end, a basic task is to find a way to prepare the ground and first-excited states (which are quasi-degenerate) of the Ising chain.

III. EFFECTIVE HAMILTONIAN

In this section, we aim to establish the connection between a single spin and a Ising chain. We will provide a way to generate the ground and first-excited states of an $(N+1)$ -site Ising chain from that of the N -site one. To proceed, we consider a system which is consisted of two parts, an Ising chain and a single spin. The Hamiltonian has the form

$$H^{(N+1)} = H_0 + H', \quad (11)$$

$$H_0 = J \sum_{i=1}^{N-1} \sigma_i^x \sigma_{i+1}^x + g \sum_{i=1}^N \sigma_i^z + g \sigma_{N+1}^z, \quad (12)$$

with $0 < g \ll J$ and the coupling between them is Ising type

$$H' = \lambda \sigma_N^x \sigma_{N+1}^x, \quad (13)$$

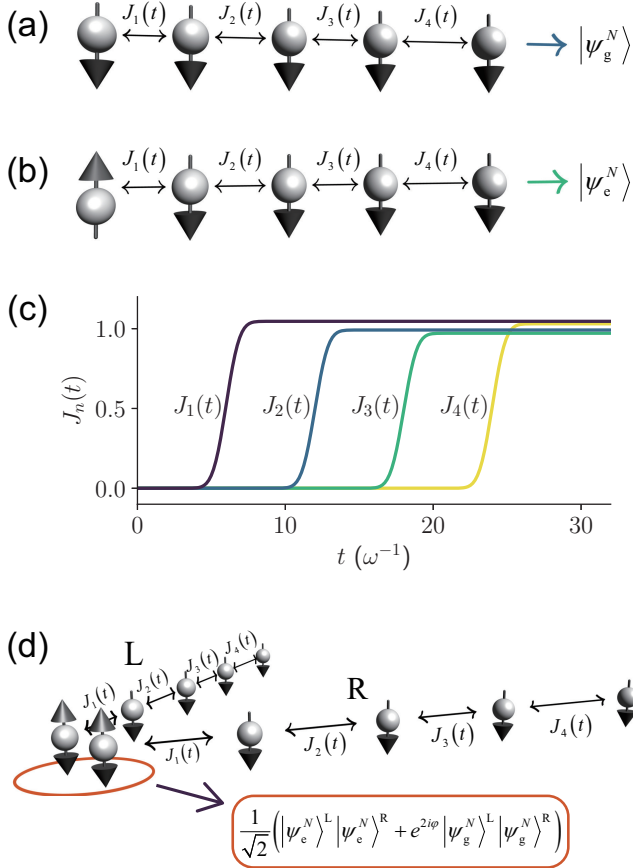


FIG. 1. Panels (a) and (b) are the schematic illustrations of dynamic crystallization process. The spin configurations in panels (a) and (b) are adiabatically evolving into the ground and first-excited state, respectively, by turning on the couplings $\{J_n(t)\}$ one by one adiabatically. (c) Plot of the couplings in the form of Eq. (27) as functions of time t . Here we take $\omega = 0.001$, $\tau = 6$, and $\lambda_n \approx 1$ as an example. (d) Schematic illustration of the entanglement transfer process between a pair of spins and two separable Ising chains.

with positive parameter $\lambda \ll J$. Here the N -site Ising chain $H_0 - g\sigma_{N+1}^z$ has gapped low-lying eigenstates $|\psi_e^N\rangle$ and $|\psi_g^N\rangle$ with energy $E_e^{(N)}$ and $E_g^{(N)}$, respectively, and the gap is sufficiently large, so that $H' = \lambda(\sigma_N^+ + \sigma_N^-)(\sigma_{N+1}^+ + \sigma_{N+1}^-)$ can be regarded as perturbation. By adiabatically eliminating the excited levels, we obtain an effective Hamiltonian

$$H_{\text{eff}}^{(N+1)} = J_{\text{eff}}^{(N)} \sigma_0^x \sigma_{N+1}^x + g_{\text{eff}}^{(N)} \sigma_0^z + g \sigma_{N+1}^z + \frac{E_e^{(N)} + E_g^{(N)}}{2}, \quad (14)$$

where the Pauli matrices σ_0^x and σ_0^z are defined as

$$\begin{aligned} \sigma_0^x |\psi_e^N\rangle &= |\psi_g^N\rangle, \quad \sigma_0^x |\psi_g^N\rangle = |\psi_e^N\rangle, \\ \sigma_0^z |\psi_e^N\rangle &= |\psi_e^N\rangle, \quad \sigma_0^z |\psi_g^N\rangle = -|\psi_g^N\rangle. \end{aligned} \quad (15)$$

And the effective coupling and field are

$$\begin{aligned} J_{\text{eff}}^{(N)} &= \lambda \langle \psi_g^N | (\sigma_N^+ + \sigma_N^-) | \psi_e^N \rangle, \\ g_{\text{eff}}^{(N)} &= \frac{E_e^{(N)} - E_g^{(N)}}{2}. \end{aligned} \quad (16)$$

The effective Hamiltonian $H_{\text{eff}}^{(N+1)}$ is a modified two-site Ising model if $g_{\text{eff}}^{(N)} \neq g$, describing low-lying eigenstates of the original Hamiltonian $H^{(N+1)}$ in Eq. (11).

It is readily to obtain the ground and first-excited states of the effective Hamiltonian $H_{\text{eff}}^{(N+1)}$, which are

$$|\psi_{\text{eff}}^g\rangle = \frac{1}{\sqrt{1 + (\xi_N^+)^2}} (|\psi_g^N\rangle |\downarrow\rangle_{N+1} - \xi_N^+ |\psi_e^N\rangle |\uparrow\rangle_{N+1}) \quad (17)$$

and

$$|\psi_{\text{eff}}^e\rangle = \frac{1}{\sqrt{1 + (\xi_N^-)^2}} (|\psi_e^N\rangle |\downarrow\rangle_{N+1} - \xi_N^- |\psi_g^N\rangle |\uparrow\rangle_{N+1}), \quad (18)$$

with energies

$$E_{\text{eff}}^g = \frac{E_e^{(N)} + E_g^{(N)}}{2} - \Lambda_N^+ \quad (19)$$

and

$$E_{\text{eff}}^e = \frac{E_e^{(N)} + E_g^{(N)}}{2} - \Lambda_N^-, \quad (20)$$

respectively, where the coefficients

$$\begin{aligned} \xi_N^\pm &= \frac{J_{\text{eff}}^{(N)}}{g \pm g_{\text{eff}}^{(N)} + \Lambda_N^\pm}, \\ \Lambda_N^\pm &= \sqrt{\left[g \pm g_{\text{eff}}^{(N)}\right]^2 + \left[J_{\text{eff}}^{(N)}\right]^2}. \end{aligned} \quad (21)$$

We note that in the case of

$$g \pm g_{\text{eff}}^{(N)} > 0, \quad (22)$$

the ground and first-excited states reduce to $|\psi_g^N\rangle |\downarrow\rangle_{N+1}$ and $|\psi_e^N\rangle |\downarrow\rangle_{N+1}$, respectively, as $J_{\text{eff}}^{(N)} = 0$. It is crucial for the present work. A straightforward conclusion is that the ground and first-excited states $|\psi_g^{N+1}\rangle$ and $|\psi_e^{N+1}\rangle$ of an $(N+1)$ -site chain can be obtained by adding a down spin $|\downarrow\rangle_{N+1}$, and then adiabatically increasing λ from 0 to J . The explicit expressions are

$$\mathcal{U}(H') |\psi_g^N\rangle |\downarrow\rangle_{N+1} = |\psi_g^{N+1}\rangle, \quad (23)$$

$$\mathcal{U}(H') |\psi_e^N\rangle |\downarrow\rangle_{N+1} = |\psi_e^{N+1}\rangle, \quad (24)$$

where

$$\mathcal{U}(H') = \mathcal{T} \exp \left[-i \int_0^\infty H'(t) dt \right], \quad (25)$$

is the propagator of the Hamiltonian $H'(t) = \lambda(t) \sigma_N^x \sigma_{N+1}^x$, with $\lambda(t)$ being a very slow function as an adiabatic passage, fulfilling $\lambda(0) = 0$ and $\lambda(\infty) = J$. Here, \mathcal{T} is the time-ordering operator.

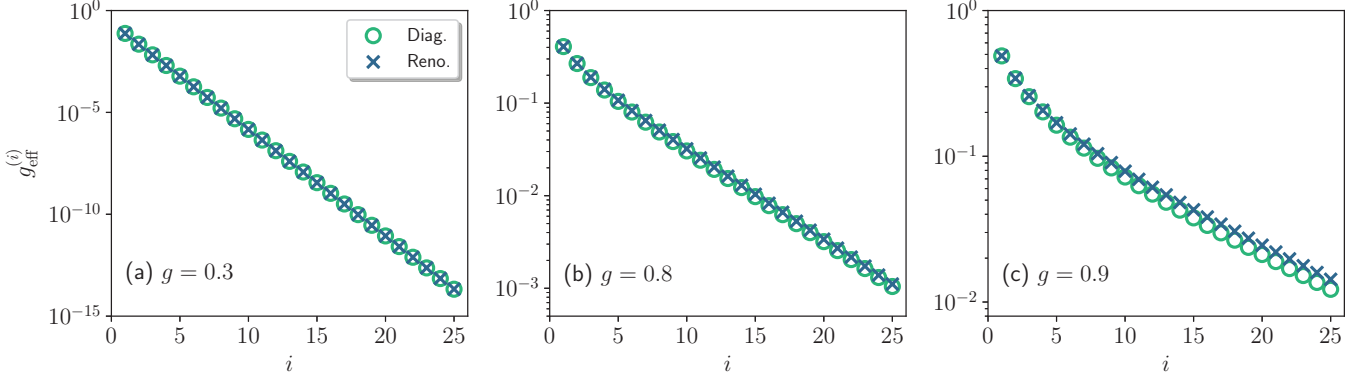


FIG. 2. Comparison of the strength of effective field $g_{\text{eff}}^{(i)}$ in Eq. (29) obtained from the renormalization method and the exact diagonalization method. The parameters are $g_i = g = 0.3, 0.8$ and 0.9 ($i \neq 1$) for panels (a), (b) and (c), respectively. Other parameters are $J_i = \lambda = 1$ and $g_1 = 0.9g$. We can see that for the case of $g \ll 1$, the two methods yield the same result.

IV. DYNAMIC CRYSTALLIZATION

So far, we have shown how to map the ground and first-excited states of an N -site Ising chain to that of $(N+1)$ -site system. It may provide a way to generate the ground and first-excited states of finite-size chain from simple spin configurations by the process of dynamic crystallization. Here, we refer to this process as "crystallization" due to the following reasons: (i) the process is about the non-interacting particles evolve to the coupled array, (ii) the final state is determined by the initial state of the first site as a seed crystal. The schematic illustration of this process is shown in Figs. 1(a) and (b) for a 5-site system.

We describe such a process by a time-dependent Hamiltonian

$$H_{\text{DC}}(t) = \sum_{i=1}^{N-1} J_i(t) \sigma_i^x \sigma_{i+1}^x + \sum_{i=1}^N g_i \sigma_i^z, \quad (26)$$

where $\{J_n(t)\}$ is a series of step-like functions to switch the couplings along the chain one by one consecutively. A typical form of $\{J_n(t)\}$ is the error function

$$J_n(t) = \frac{\lambda_n}{2} \{ \text{erf} [\omega(t - n\tau)] + 1 \}, \quad (27)$$

where λ_n is the strength of final coupling. The shape of function $J_n(t)$ is plotted in Fig. 1(c). In the following, we estimate the possible result, based on the renormalization method. The basic idea is as following. According to the analysis in the previous section, in the adiabatic regime, the dynamics in the duration of switching on J_i is governed approximately by the effective Hamiltonian in the form

$$H_{\text{eff}}^{(i+1)} = J_{\text{eff}}^{(i)} \sigma_0^x \sigma_{i+1}^x + g_{\text{eff}}^{(i)} \sigma_0^z + g_{i+1} \sigma_{i+1}^z + \frac{E_{\text{eff}}^{\text{e}(i)} + E_{\text{eff}}^{\text{g}(i)}}{2}, \quad (28)$$

where Pauli operators σ_0^x and σ_0^z take actions on the ground and first-excited states of i -site chain, parameters $J_{\text{eff}}^{(i)}$, $g_{\text{eff}}^{(i)}$, $E_{\text{eff}}^{\text{e}(i)}$, and $E_{\text{eff}}^{\text{g}(i)}$ are obtained from $H_{\text{eff}}^{(i)}$.

Then $H_{\text{eff}}^{(i+1)}$ generates the parameters in the effective Hamiltonian $H_{\text{eff}}^{(i+2)}$:

$$\begin{aligned} g_{\text{eff}}^{(i+1)} &= \frac{E_{\text{eff}}^{\text{e}(i+1)} - E_{\text{eff}}^{\text{g}(i+1)}}{2} \\ &= \frac{1}{2} (\Lambda_i^+ - \Lambda_i^-) \end{aligned} \quad (29)$$

and

$$\begin{aligned} J_{\text{eff}}^{(i+1)} &= \lambda_i \left\langle \psi_{\text{eff}}^{\text{g}(i+1)} \right| (\sigma_{i+1}^+ + \sigma_{i+1}^-) \left| \psi_{\text{eff}}^{\text{e}(i+1)} \right\rangle \\ &= -\frac{\lambda_i (\xi_i^+ + \xi_i^-)}{\sqrt{1 + (\xi_i^+)^2} \sqrt{1 + (\xi_i^-)^2}}. \end{aligned} \quad (30)$$

We start from $i = 1$ with $J_{\text{eff}}^{(1)} = \lambda_1$, $g_{\text{eff}}^{(1)} = g_1$, and $E_{\text{eff}}^{\text{e}(1)} = -E_{\text{eff}}^{\text{g}(1)} = g_1$, i.e.,

$$H_{\text{eff}}^{(2)} = \lambda_1 \sigma_1^x \sigma_2^x + g_1 \sigma_1^z + g_2 \sigma_2^z, \quad (31)$$

which is a 2-site Ising model. Then effective parameters $g_{\text{eff}}^{(i)}$ and $J_{\text{eff}}^{(i)}$ with $i > 1$ are obtained by the iteration method from Eqs. (29) and (30) or $H_{\text{eff}}^{(i)}$. In order to verify the proposed approximation approach, we compare the strength of effective field $g_{\text{eff}}^{(i)}$ obtained from the renormalization method in Eq. (29) and the exact diagonalization method. The plots in Fig. 2 show that two methods yield the same result for small g .

Importantly, when a set of obtained parameters $\{g_{\text{eff}}^{(i)}\}$ satisfy the condition

$$g_{i+1} - g_{\text{eff}}^{(i)} > 0, \quad (32)$$

we have

$$\mathcal{U}(H_{\text{DC}}) (\alpha |\uparrow\rangle_1 + \beta |\downarrow\rangle_1) \prod_{l=2}^N |\downarrow\rangle_l = \alpha |\psi_e^N\rangle + e^{i\varphi} \beta |\psi_g^N\rangle, \quad (33)$$

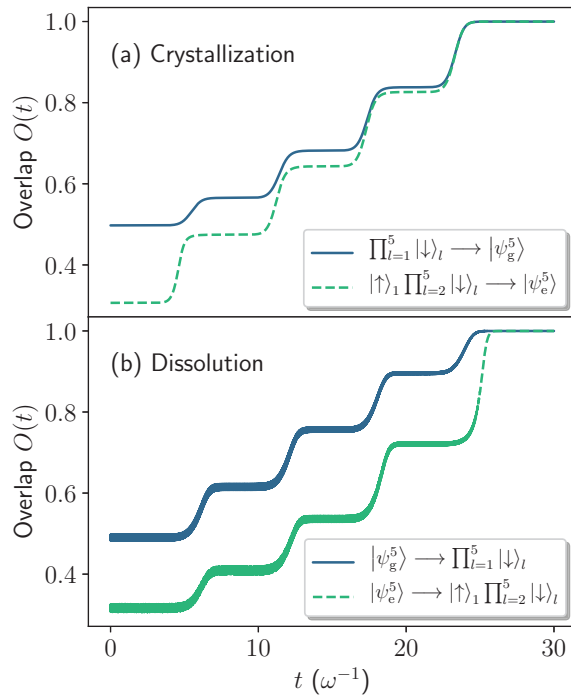


FIG. 3. Numerical results of the overlaps between target states and evolved states for a 5-site Ising chain. In the legends, the initial (target) states are on the left (right) side of the arrows. (a) The dynamic crystallization process. The ground (first-excited) state is generated through numerical diagonalization for a uniform Ising chain with parameters $J = 1$, $g = 0.4$ and $N = 5$. The time-dependent Hamiltonian is taken as the form in Eq. (26) with the couplings $\{J_n(t)\}$ in the form of Eq. (27). The parameters are $g_i = g$ ($i \neq 1$), $g_1 = 0.9g$, $\omega = 0.001$, $\tau = 6$, and $\lambda_n = 1$. (b) The dynamic dissolution process, which can be regarded as a time reversal of the crystallization process. In contrast to the crystallization process, here the initial state is taken as ground (first-excited) state of the Ising chain, and the couplings $\{J_n(t)\}$ are removed one by one adiabatically.

where $\mathcal{U}(H_{DC}) = \mathcal{T} \exp \left[-i \int_0^\infty H_{DC}(t) dt \right]$, and φ is a dynamical phase. This process is similar to that of dynamic crystallization in the case $\alpha = 0$ or $\beta = 0$. Here the first spin at state $|\uparrow\rangle_1 (|\downarrow\rangle_1)$ takes the role of a seed crystal, which determines the state $|\psi_e^N\rangle (|\psi_g^N\rangle)$ of the crystal with large N . We demonstrate the dynamic crystallization by numerical simulation in finite-size system. We use the overlap $O(t) = |\langle \Psi_T | \Psi(t) \rangle|$ between target state $|\Psi_T\rangle = |\psi_g^N\rangle (|\psi_e^N\rangle)$ and evolved state

$$|\Psi(t)\rangle = \mathcal{T} \exp \left[-i \int_0^t H_{DC}(t') dt' \right] |\Psi(0)\rangle, \quad (34)$$

where $|\Psi(0)\rangle = |\downarrow\rangle_1 (|\uparrow\rangle_1) \prod_{l=2}^N |\downarrow\rangle_l$, to measure the efficiency of the process. The overlaps $O(t)$ are plotted in Fig. 3(a). Meanwhile, as a time reversal of the crystallization process, the simulation for the dissolution process is also performed [see Fig. 3(b)], where

the corresponding states are $|\Psi(0)\rangle = |\psi_g^N\rangle (|\psi_e^N\rangle)$ and $|\Psi_T\rangle = |\downarrow\rangle_1 (|\uparrow\rangle_1) \prod_{l=2}^N |\downarrow\rangle_l$. Here the computation is performed by using a uniform mesh in the time discretization for the time-dependent Hamiltonian $H_{DC}(t)$. The result accords with our prediction for both processes.

We would like to point out that the dynamic crystallization process cannot map a qubit state onto a many-qubit two-level state due to the uncertainty of the phase φ . However, as an application in quantum information processing, this makes it possible to realize the entanglement transfer from a pair of qubits to two independent Ising chains, as macroscopic objects. Entanglement is considered to be one of the most profound features of quantum mechanics [28, 29] and a very powerful resource for quantum information processing and communication. Specifically, robust and long-lived entanglement of material objects is a desirable task in quantum information processing, including teleportation of quantum states of matter and quantum memory [30]. Here we propose a scheme to generate robust entanglement between two quantum spin chains, as macroscopic objects.

The system we concern is a simple extension of the original system, described by the Hamiltonian

$$H_D = H^L + H^R, \quad (35)$$

where H^L and H^R represent two independent but identical Ising chains described by Eq. (1), respectively. Consider an initial state, in which the first two spins are maximally entangled, being state $(|\uparrow\rangle_1^L |\uparrow\rangle_1^R + |\downarrow\rangle_1^L |\downarrow\rangle_1^R) / \sqrt{2}$. Applying the process in Eq. (33), we have

$$\begin{aligned} & \frac{1}{\sqrt{2}} \mathcal{U}(H_D) \left(|\uparrow\rangle_1^L |\uparrow\rangle_1^R + |\downarrow\rangle_1^L |\downarrow\rangle_1^R \right) \prod_{l=2}^N |\downarrow\rangle_l^L \prod_{l=2}^N |\downarrow\rangle_l^R \\ &= \frac{1}{\sqrt{2}} \left(|\psi_e^N\rangle^L |\psi_e^N\rangle^R + e^{i2\varphi} |\psi_g^N\rangle^L |\psi_g^N\rangle^R \right). \end{aligned} \quad (36)$$

It represents entanglement transfer from two spins to two independent Ising chains, keeping the maximal concurrence no matter what the value of φ . Such a process is schematically illustrated in Fig. 1(d).

V. QUENCHED DISORDERED PERTURBATION AND ENTANGLEMENT DISTILLATION

In this section, we focus on the many-particle qubit in two aspects. (i) We demonstrate the robustness of the macroscopic qubit state in the presence of quenched disordered perturbation via a numerical simulation in finite systems. (ii) We propose a scheme to distill the entanglement of two Ising chains via a dissolution process, which transfers the entanglement from chains to a fixed pair of spins.

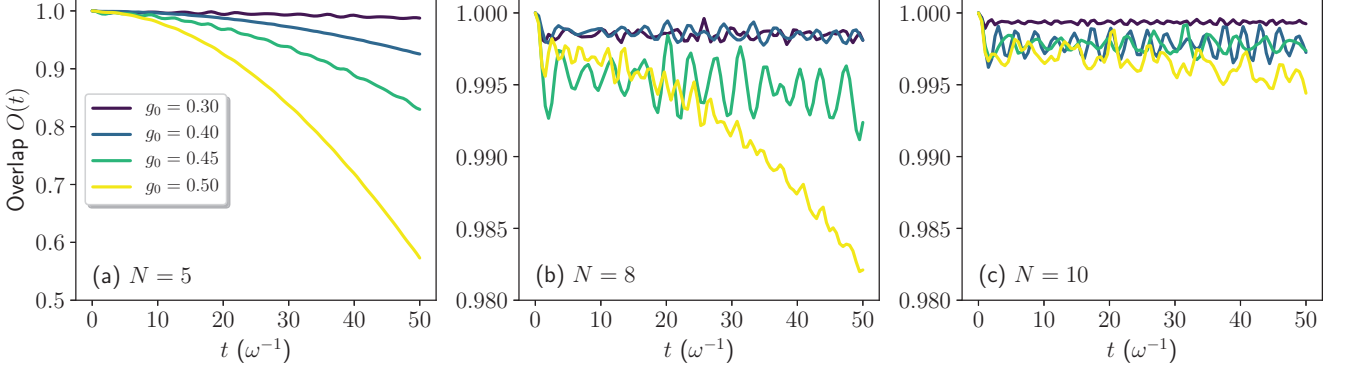


FIG. 4. Numerical results of the overlap between the initial state $|\Psi(0)\rangle$ and its evolved states $|\Psi(t)\rangle$ under quenched disordered perturbation with different N and g_0 . The sizes of the chains are $N = 5$, $N = 8$ and $N = 10$ for panels (a), (b) and (c), respectively. The disorder strength is $R = 0.2$ and the parameters of the uniform Hamiltonian H are $J_j = 1$ and $g_j = g_0$. Other parameters are $\alpha = \beta = 1/\sqrt{2}$ and $\omega = 1$.

A. Quenched disordered perturbation

The advantage of the proposed many-particle qubit, the quasi-degenerate ground states of Ising chain, is robust against local perturbation. Technically speaking, there always exists a D_N operator even parameters J_j and g_j are slightly random (see Appendix). It means that the degeneracy cannot be lifted when the random perturbation is induced adiabatically. Then during the process, $\alpha |\psi_e^N(0)\rangle + \beta |\psi_g^N(0)\rangle$ evolves to $\alpha |\psi_e^N(t)\rangle + \beta |\psi_g^N(t)\rangle$, without extra time-dependent phase difference on α and β , keep the original quantum information. Here $|\psi_g^N(t)\rangle$ and $|\psi_e^N(t)\rangle$ are instantaneous ground and first-excited eigenstates of the time-dependent Hamiltonian. However, in practice, the appearance of disordered perturbation from the environment is random in time. In the following we consider an extreme case, in which a disordered perturbation is added as a quenching process, and investigate the effect of quenched disordered perturbation on a many-spin qubit initial state $|\Psi(0)\rangle = \alpha |\psi_e^N(0)\rangle + \beta |\psi_g^N(0)\rangle$ by employ numerical simulation for the time evolution on finite N system. We add a time-dependent perturbation H_{Ran} to the uniform N -site Ising chain. Here H_{Ran} takes the form

$$H_{\text{Ran}} = \sum_{j=1}^{N-1} \Delta J_j \sigma_j^x \sigma_{j+1}^x + \sum_{j=1}^N \Delta g_j \sigma_j^z, \quad (37)$$

in which the parameters take the Heaviside function of time

$$\Delta J_j = \Delta g_j = \frac{\Delta_j^R}{2} [\text{sgn}(t) + 1]. \quad (38)$$

Here Δ_j^R denotes a uniform random number within the interval $(-R, R)$, taking the role of the disorder strength. We still use the overlap $O(t) = |\langle \Psi(0) | \Psi(t) \rangle|$ between $|\Psi(0)\rangle$ and evolved state

$$|\Psi(t)\rangle = \exp[-i(H + H_{\text{Ran}})t] |\Psi(0)\rangle, \quad (39)$$

to measure the influence of the quenched perturbation. The overlap $O(t)$ for systems with different size and parameters are plotted in Fig. 4. The result shows that for a fixed random strength R , (i) for a fixed N , larger g_0 leads to smaller fidelity, (ii) while for a fixed g_0 , larger N leads to larger fidelity. It indicates that even for finite size system with $N = 10$, the ground and first-excited states are very robust for the case with not large $g_0 < 0.5$.

B. Entanglement distillation

In the following, we turn to demonstrate an adiabatic passage for entanglement distillation from an obtained macroscopic entangled state. To this end, we employ numerical simulation for the time evolution on finite N -site system H in Eq. (1). We start from an initial state $|\Psi(0)\rangle = \alpha |\psi_e^N(0)\rangle + \beta |\psi_g^N(0)\rangle$. At first step, an arbitrary target spin at site l is selected by decreasing the local field g_l to zero, adiabatically. At second step, after g_l vanishing, we remove the coupling J_j one by one, adiabatically. The order of the dissolution is $J_1 \rightarrow 0$, $J_2 \rightarrow 0, \dots, J_{l-1} \rightarrow 0$, and then $J_N \rightarrow 0$, $J_{N-1} \rightarrow 0, \dots, J_l \rightarrow 0$. The above parameters as functions of time are plotted in Figs. 5(a) and (b) for a 5-site system. During this process, we monitor the evolved state of the spin at site l , by its 2×2 reduced density matrix

$$\rho_l(t) = \text{Tr}_{(l)} [|\Psi(t)\rangle \langle \Psi(t)|], \quad (40)$$

where $\text{Tr}_{(l)} [\dots]$ denotes taking the trace over all the rest of the freedom. For the initial state $|\Psi(0)\rangle$, the target qubit state is $\alpha |\uparrow\rangle_l + e^{i\varphi} \beta |\downarrow\rangle_l$, which is equivalent to the density matrix $\bar{\rho}_l = \alpha \alpha^* |\uparrow\rangle_l \langle \uparrow|_l + \beta \beta^* |\downarrow\rangle_l \langle \downarrow|_l + e^{-i\varphi} \alpha \beta^* |\uparrow\rangle_l \langle \downarrow|_l + e^{i\varphi} \beta \alpha^* |\downarrow\rangle_l \langle \uparrow|_l$. To describe the efficiency, we employ the trace distance

$$T_l(t) = \frac{1}{2} \text{Tr} \left[\sqrt{[\bar{\rho}_l - \rho_l(t)]^2} \right], \quad (41)$$

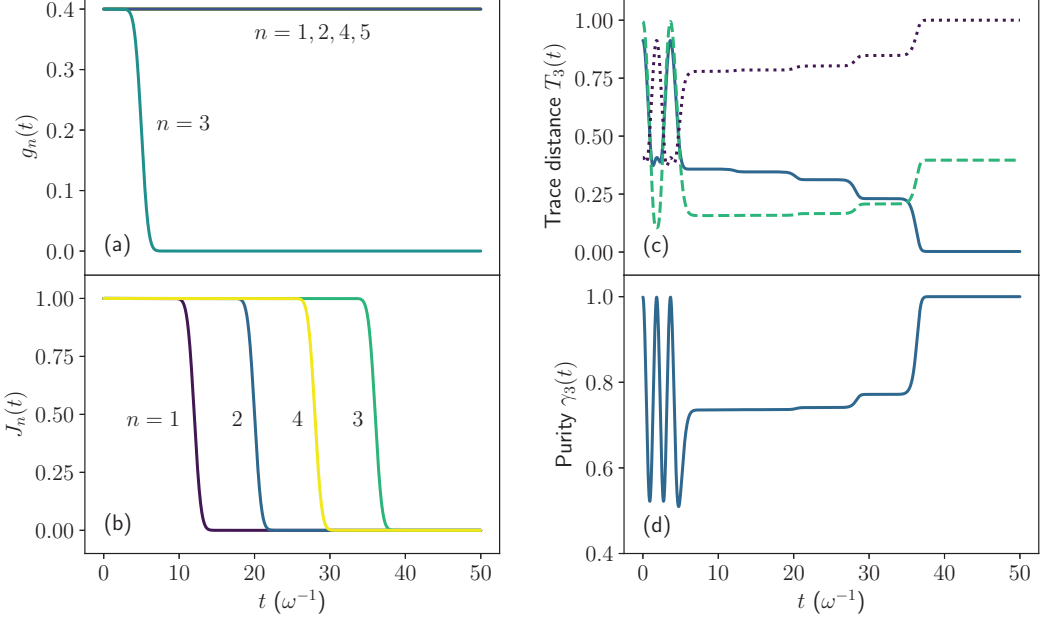


FIG. 5. (a) Adiabatic change of the strength of field $g_n(t)$. The target spin at site $l = 3$ is selected by decreasing the local field g_3 to 0 adiabatically. (b) Adiabatic change of the strength of coupling $J_n(t)$. (c) The trace distance defined in Eq. (41) for different target qubit state $\bar{\rho}_l$ at site $l = 3$. The solid, dashed and dotted lines represent the results of target qubit states with different phase factors $\varphi = -0.82i, 0$ and $(\pi - 0.82i)$, respectively. (d) Purity of the reduced density matrix $\rho_l(t)$ for site $l = 3$ defined in Eq. (42). Other parameters are $N = 5$, $\alpha = \beta = 1/\sqrt{2}$ and $\omega = 0.01$.

which is a measure of the distinguishability between the evolved and target states. We note that the final state $\rho_l(t)$ depends on the adiabatic passage due to the extra dynamic phase φ . Therefore, even though state $\rho_l(t)$ does not meet $\bar{\rho}_l$, it can still be a pure state. We have known that this fact makes it possible for entanglement transfer as mentioned in Eq. (33). Then it is important to measure the purity of the reduced density matrix $\rho_l(t)$, which is defined as

$$\gamma_l(t) = \text{Tr} [\rho_l(t)^2]. \quad (42)$$

The numerical results plotted in Figs. 5(c) and (d) show that the trace distance $T_l(t)$ and purity $\gamma_l(t)$ as functions of time accord to our prediction, i.e.,

$$\mathcal{U}(H)(\alpha |\psi_e^N\rangle + \beta |\psi_g^N\rangle) = (\alpha |\uparrow\rangle_l + e^{i\varphi} \beta |\downarrow\rangle_l) \prod_{j \neq l}^N |\downarrow\rangle_j, \quad (43)$$

which is crucial to the scheme of entanglement distillation in the following.

Now we extend the result in Eq. (43) to the two-chain system $H_D = H^L + H^R$. We focus on the entanglement distillation of two-spin system from two entangled Ising chains. For simplicity, we consider the case with $\alpha = \beta =$

$1/\sqrt{2}$. From Eq. (43) we have

$$\begin{aligned} & \frac{1}{\sqrt{2}} \mathcal{U}(H_{L,R}) (|\psi_e^N\rangle^{L,R} \pm |\psi_g^N\rangle^{L,R}) \\ &= \frac{1}{\sqrt{2}} (|\uparrow\rangle_l^{L,R} \pm e^{i\varphi} |\downarrow\rangle_l^{L,R}) \prod_{j \neq l}^N |\downarrow\rangle_j^{L,R}, \end{aligned} \quad (44)$$

which results in

$$\begin{aligned} & \frac{1}{\sqrt{2}} \mathcal{U}(H_D) (|\psi_e^N\rangle^L |\psi_e^N\rangle^R + |\psi_g^N\rangle^L |\psi_g^N\rangle^R) \\ &= \frac{1}{\sqrt{2}} (|\uparrow\rangle_l^L |\uparrow\rangle_l^R + e^{i2\varphi} |\downarrow\rangle_l^L |\downarrow\rangle_l^R) \prod_{j \neq l}^N |\downarrow\rangle_j^L \prod_{j \neq l}^N |\downarrow\rangle_j^R \end{aligned} \quad (45)$$

by direct derivation. Accordingly, it also provides a way to transfer the maximal pair-entanglement from location i to l ,

$$\begin{aligned} & \frac{1}{\sqrt{2}} (|\uparrow\rangle_i^L |\uparrow\rangle_i^R + |\downarrow\rangle_i^L |\downarrow\rangle_i^R) \\ & \rightarrow \frac{1}{\sqrt{2}} (|\uparrow\rangle_l^L |\uparrow\rangle_l^R + e^{i\varphi'} |\downarrow\rangle_l^L |\downarrow\rangle_l^R). \end{aligned} \quad (46)$$

VI. DISCUSSION

In this paper, we have studied the relationship between the gapped quasi-degenerate ground states of an N -site Ising chain and that of the $(N + 1)$ -site chain,

based on which the real-space renormalization method is developed. It allows us to build the effective Hamiltonian, which is an exactly solvable modified 2-site Ising model and captures the low-energy physics of a given system. Numerical calculation shows that such an effective Hamiltonian has higher efficiency and is a feasible method for large-size system. Due to the protection of energy gap, this approximate description provides an alternative way to prepare the ground state and first-excited state of an Ising chain on demand by dynamic process of crystallization, generating robust macroscopic quantum states against disordered perturbation. To demonstrate the potential application of our finding, we proposed a scheme of entanglement transfer between a pair of qubits and two Ising chains, as macroscopic topological qubits. Our work, including the numerical result for small size system, reveals that transverse field Ising chains can be utilized for developing inherently robust artificial devices for topological quantum information processing and communication.

ACKNOWLEDGMENT

This work was supported by the National Natural Science Foundation of China (under Grant No. 11874225).

APPENDIX

In this appendix, we will show the method of obtaining the nonlocal spin operator D_N in Eq. (4). Starting from the Ising chain H in Eq. (1) with uniform parameters $J_j = J$ and $g_j = g$, we first perform the Jordan-Wigner transformation [31]

$$\begin{aligned}\sigma_j^x &= \prod_{l < j} \left(1 - 2c_l^\dagger c_l\right) \left(c_j + c_j^\dagger\right), \\ \sigma_j^y &= i \prod_{l < j} \left(1 - 2c_l^\dagger c_l\right) \left(c_j - c_j^\dagger\right), \\ \sigma_j^z &= 2c_j^\dagger c_j - 1,\end{aligned}\quad (A1)$$

to replace the Pauli operators by the fermionic operators c_j . The Hamiltonian is transformed to a well known Kitaev model

$$\begin{aligned}H_{\text{Kitaev}} &= J \sum_{j=1}^{N-1} \left(c_j^\dagger c_{j+1} + c_j^\dagger c_{j+1}^\dagger\right) + \text{H.c.} \\ &+ g \sum_{j=1}^N \left(2c_j^\dagger c_j - 1\right).\end{aligned}\quad (A2)$$

To get the solution of the model, we then introduce the Majorana fermion operators

$$a_j = c_j^\dagger + c_j, b_j = -i \left(c_j^\dagger - c_j\right), \quad (A3)$$

which satisfy the commutation relations

$$\begin{aligned}\{a_j, a_{j'}\} &= 2\delta_{j,j'}, \{b_j, b_{j'}\} = 2\delta_{j,j'}, \\ \{a_j, b_{j'}\} &= 0.\end{aligned}\quad (A4)$$

Then the Majorana representation of the original Hamiltonian is

$$H_M = \frac{i}{2} J \sum_{j=1}^{N-1} b_j a_{j+1} - \frac{i}{2} g \sum_{j=1}^N a_j b_j + \text{H.c.}, \quad (A5)$$

the core matrix of which is that of a $2N$ -site SSH chain in single-particle invariant subspace. Based on the exact diagonalization result of the SSH chain, the Hamiltonian H_{Kitaev} can be written as the diagonal form

$$H_{\text{Kitaev}} = \sum_{n=1}^N \varepsilon_n (d_n^\dagger d_n - \frac{1}{2}). \quad (A6)$$

Here d_n is a fermionic operator, satisfying $\{d_n, d_{n'}\} = 0$, and $\{d_n, d_{n'}^\dagger\} = \delta_{n,n'}$. On the other hand, we have the relations

$$[d_n, H_{\text{Kitaev}}] = \varepsilon_n d_n, [d_n^\dagger, H_{\text{Kitaev}}] = -\varepsilon_n d_n^\dagger, \quad (A7)$$

which result in the mapping between the eigenstates of H_{Kitaev} . Direct derivation show that, for an arbitrary eigenstate $|\psi\rangle$ of H_{Kitaev} with eigenenergy E , i.e.,

$$H_{\text{Kitaev}} |\psi\rangle = E |\psi\rangle, \quad (A8)$$

state $d_n |\psi\rangle$ ($d_n^\dagger |\psi\rangle$) is also an eigenstate of H_{Kitaev} with the eigenenergy $E - \varepsilon_n$ ($E + \varepsilon_n$), i.e.,

$$H_{\text{Kitaev}} (d_n |\psi\rangle) = (E - \varepsilon_n) (d_n |\psi\rangle) \quad (A9)$$

and

$$H_{\text{Kitaev}} (d_n^\dagger |\psi\rangle) = (E + \varepsilon_n) (d_n^\dagger |\psi\rangle), \quad (A10)$$

if $d_n |\psi\rangle \neq 0$ ($d_n^\dagger |\psi\rangle \neq 0$).

In large N limit, and within the topologically nontrivial region $|g/J| < 1$ ($g \neq 0$), the edge modes appear with $\varepsilon_N = 0$ and the edge operator d_N can be expressed as

$$\begin{aligned}d_N &= \frac{1}{2} \sqrt{1 - \left(\frac{g}{J}\right)^2} \sum_{j=1}^N \left\{ \left[\left(-\frac{g}{J}\right)^{j-1} + \left(-\frac{g}{J}\right)^{N-j} \right] c_j^\dagger \right. \\ &\quad \left. + \left[\left(-\frac{g}{J}\right)^{j-1} - \left(-\frac{g}{J}\right)^{N-j} \right] c_j \right\},\end{aligned}\quad (A11)$$

i.e., d_N is a linear combination of particle and hole operators of spinless fermions c_j on the edge, and we have $[d_N, H_{\text{Kitaev}}] = \varepsilon_N d_N = 0$. Furthermore, applying the inverse Jordan-Wigner transformation, d_N can be expressed as the combination of spin operators,

$$\begin{aligned}D_N &= \frac{1}{2} \sqrt{1 - \left(\frac{g}{J}\right)^2} \sum_{j=1}^N \prod_{l < j} (-\sigma_l^z) \\ &\quad \times \left[\left(-\frac{g}{J}\right)^{j-1} \sigma_j^x - i \left(-\frac{g}{J}\right)^{N-j} \sigma_j^y \right],\end{aligned}\quad (A12)$$

In fact, d_N and D_N are identical, but only in different representations. Thus, from $[d_N, H_{\text{Kitaev}}] = 0$, we have

$$[D_N, H] = [D_N^\dagger, H] = 0, \quad (\text{A13})$$

which lead to the degeneracy of the eigenstates. Furthermore, from the canonical commutation relations $\{d_N, d_N^\dagger\} = 1$ and $\{d_N, d_N\} = 0$, we have

$$\{D_N, D_N^\dagger\} = 1, (D_N)^2 = (D_N^\dagger)^2 = 0. \quad (\text{A14})$$

For the Ising chain with slight disordered deviations on the uniform J and g , the operator D_N still exists, which has the form

$$D_N = \Omega \sum_{j=1}^N \prod_{l < j} (-\sigma_l^z) (h_j^+ \sigma_j^x - i h_j^- \sigma_j^y), \quad (\text{A15})$$

since the edge mode of SSH chain in Eq. (A5) is robust against disordered perturbation. Here the coefficients Ω and h_j^\pm can be obtained by diagonalization of the SSH chain with slight disordered deviations on the uniform $J_j = J$ and $g_j = g$. It can be check that the commutation relations in Eqs. (A13) and (A14) still hold for the operator D_N with disordered perturbation, as long as the edge mode of SSH chain with zero energy exists.

[1] S. Sachdev, *Quantum Phase Transitions* (Cambridge University Press, Cambridge, England, 1999).

[2] G. Zhang and Z. Song, Topological characterization of extended quantum Ising models, *Phys. Rev. Lett.* **115**, 177204 (2015).

[3] G. Zhang, C. Li, and Z. Song, Majorana charges, winding numbers and Chern numbers in quantum Ising models, *Sci. Rep.* **7**, 8176 (2017).

[4] A. Y. Kitaev, Unpaired Majorana fermions in quantum wires, *Phys. Usp.* **44**, 131 (2001).

[5] R. Botet, R. Jullien, and M. Kolb, Finite-size-scaling study of the spin-1 Heisenberg-Ising chain with uniaxial anisotropy, *Phys. Rev. B* **28**, 3914 (1983).

[6] M. P. Nightingale, and H. W. J. Blöte, Gap of the linear spin-1 Heisenberg antiferromagnet: A Monte Carlo calculation, *Phys. Rev. B* **33**, 659(R) (1986).

[7] S. R. White and D. A. Huse, Numerical renormalization-group study of low-lying eigenstates of the antiferromagnetic $S = 1$ Heisenberg chain, *Phys. Rev. B* **48**, 3844 (1993).

[8] S. R. White and I. Affleck, Spectral function for the $S = 1$ Heisenberg antiferromagnetic chain, *Phys. Rev. B* **77**, 134437 (2008).

[9] Y. P. Shim, A. Sharma, C. Y. Hsieh, and P. Hawrylak, Artificial Haldane gap material on a semiconductor chip, *Solid State Commun.* **150**, 2065 (2010).

[10] F. Delgado, C. D. Batista and J. Fernández-Rossier, Local probe of fractional edge states of $S = 1$ Heisenberg spin chains, *Phys. Rev. Lett.* **111**, 167201 (2013).

[11] W. J. L. Buyers, R. M. Morra, R. L. Armstrong, M. J. Hogan, P. Gerlach, and K. Hirakawa, Experimental evidence for the Haldane gap in a spin-1 nearly isotropic, antiferromagnetic chain, *Phys. Rev. Lett.* **56**, 371 (1986).

[12] R. M. Morra, W. J. L. Buyers, R. L. Armstrong, and K. Hirakawa, Spin dynamics and the Haldane gap in the spin-1 quasi-onedimensional antiferromagnet CsNiCl_3 , *Phys. Rev. B* **38**, 543 (1988).

[13] E. Čižmár, M. Ozerov, O. Ignatchik, T. P. Papageorgiou, J. Wosnitza, S. A. Zvyagin, J. Krzystek, Z. Zhou, C. P. Landee, B. R. Landry, M. M. Turnbull and J. L. Wikaira, Magnetic properties of the Haldane-gap material $[\text{Ni}(\text{C}_2\text{H}_8\text{N}_2)_2\text{NO}_2](\text{BF}_4)$, *New J. Phys.* **10**, 033008 (2008).

[14] C. Rüegg, N. Cavadini, A. Furrer, H.-U. Güdel, K. Krämer, H. Mutka, A. Wildes, K. Habicht and P. Vorderwisch, Bose-Einstein condensation of the triplet states in the magnetic insulator TlCuCl_3 , *Nature* **423**, 62–65 (2003).

[15] H. M. Rønnow, R. Parthasarathy, J. Jensen, G. Aeppli, T. F. Rosenbaum and D. F. McMorrow, Quantum phase transition of a magnet in a spin bath, *Science* **308**, 389–392 (2005).

[16] J. Simon, W. S. Bakr, R. Ma, M. E. Tai, P. M. Preiss and M. Greiner, Quantum simulation of antiferromagnetic spin chains in an optical lattice, *Nature (London)* **472**, 307 (2010).

[17] F. D. M. Haldane, Nonlinear Field Theory of Large-Spin Heisenberg Antiferromagnets: Semiclassically Quantized Solitons of the One-Dimensional Easy-Axis Néel State, *Phys. Rev. Lett.* **50**, 1153 (1983).

[18] I. Affleck, T. Kennedy, E. H. Lieb and H. Tasaki, Valence bond ground states in isotropic quantum antiferromagnets, *Commun. Math. Phys.* **115**, 477 (1988).

[19] I. Affleck, Quantum spin chains and the Haldane gap, *J. Phys. Condens. Matter* **1**, 3047 (1989).

[20] J. R. Petta, A. C. Johnson, J. M. Taylor, E. A. Laird, A. Yacoby, M. D. Lukin, C. M. Marcus, M. P. Hanson and A. C. Gossard, Coherent manipulation of coupled electron spins in semiconductor quantum dots, *Science* **309**, 2180–2184 (2005).

[21] M. Korkusinski, and P. Hawrylak, Coded qubits based on electron spin, in *Semiconductor quantum bits* (eds Benson, O. & Henneberger, F.) 3–32 (World Scientific, 2008).

[22] M. W. Johnson, M. H. S. Amin, S. Gildert, T. Lanting, F. Hamze, N. Dickson, R. Harris, A. J. Berkley, J. Johansson, P. Bunyk, E. M. Chapple, C. Enderud, J. P. Hilton, K. Karimi, E. Ladizinsky, N. Ladizinsky, T. Oh, I. Perminov, C. Rich, M. C. Thom, E. Tolkacheva, C. J. S. Truncik, S. Uchaikin, J. Wang, B. Wilson and G. Rose, Quantum annealing with manufactured spins, *Nature* **473**, 194–198 (2011).

[23] C.-Y. Hsieh, Y. P. Shim, M. Korkusinski, and P. Hawrylak, Physics of lateral triple quantum-dot molecules with controlled electron numbers, *Rep. Prog. Phys.* **75**, 114501 (2012).

(2012).

[24] S. D. Sarma, M. Freedman and C. Nayak, Majorana zero modes and topological quantum computation, npj Quantum Information **1**, 15001 (2015).

[25] C. Nayak, S. H. Simon, A. Stern, M. Freedman, and S. D. Sarma, Non-Abelian anyons and topological quantum computation, Rev. Mod. Phys. **80**, 1083 (2008).

[26] A. Stern, Non-Abelian states of matter, Nature (London) **464**, 187 (2010).

[27] J. Alicea, New directions in the pursuit of Majorana fermions in solid state systems, Rep. Prog. Phys. **75**, 076501 (2012).

[28] A. Einstein, B. Podolsky, and N. Rosen, N. Can Quantum-Mechanical Description of Physical Reality Be Considered Complete?, Phys. Rev. **47**, 777 (1935).

[29] J. S. Bell, *Speakable and Unspeakable in Quantum Mechanics* (Cambridge Univ. Press, Cambridge, 1988).

[30] R. Horodecki, P. Horodecki, M. Horodecki, and K. Horodecki, Quantum entanglement, Rev. Mod. Phys. **81**, 865 (2009).

[31] P. Jordan and E. Wigner, über das paulische äquivalenzverbot Z. Physik **47**, 631 (1928).